

Alan Thorne†,
Rainer Grün*,
Graham Mortimer*,
Nigel A. Spooner*,
John J. Simpson‡,
Malcolm
McCulloch*,
Lois Taylor* &
Darren Curnoe†

†*Research School of Pacific
and Asian Studies, Australian
National University, Canberra
ACT 0200, Australia. E-mail:
Thorne@coombs.anu.edu.au*

**Research School of Earth
Sciences, Australian National
University, Canberra ACT
0200, Australia. E-mail:
rainer.grun@anu.edu.au*

‡*Department of Physics,
University of Guelph, Guelph,
ONT N1G 2W1, Canada*

Australia's oldest human remains: age of the Lake Mungo 3 skeleton

We have carried out a comprehensive ESR and U-series dating study on the Lake Mungo 3 (LM3) human skeleton. The isotopic Th/U and Pa/U ratios indicate that some minor uranium mobilization may have occurred in the past. Taking such effects into account, the best age estimate for the human skeleton is obtained through the combination of U-series and ESR analyses yielding $62,000 \pm 6000$ years. This age is in close agreement with OSL age estimates on the sediment into which the skeleton was buried of $61,000 \pm 2000$ years. Furthermore, we obtained a U-series age of $81,000 \pm 21,000$ years for the calcitic matrix that was precipitated on the bones after burial. All age results are considerably older than the previously assumed age of LM3 and demonstrate the necessity for directly dating hominid remains. We conclude that the Lake Mungo 3 burial documents the earliest known human presence on the Australian continent. The age implies that people who were skeletally within the range of the present Australian indigenous population colonized the continent during or before oxygen isotope stage 4 (57,000–71,000 years).

© 1999 Academic Press


Received 16 November
1998

Revision received
25 February 1999
and accepted 7 March 1999

Keywords: Lake Mungo 3,
ESR, U-series, OSL dating.

Journal of Human Evolution (1999) **36**, 591–612

Article No. jhev.1999.0305

Available online at <http://www.idealibrary.com> on 

Introduction

On 26 February 1974 a near-complete skeleton (Figure 1) was found in an eroding grave on the backslope of the Pleistocene lunette fringing Lake Mungo, one of the now dry Willandra Lakes in western New South Wales [see Figure 2(a)]. The body of this individual, Lake Mungo 3 (LM3) had been sprinkled with powdered red ochre before the grave had been filled in. The skeletal morphology of this individual is gracile (Thorne, 1980), and it lies within the range of living Aboriginal Australians. Figure 2(b, c) shows the stratigraphic position of the burial. The stratigraphic sequence and chronology of the south end of

the “Walls of China” lunette was recently described by Bowler (1998):

Golgol: the basal sedimentary unit characterized by deep red calcareous soil, indicating prolonged pedogenesis and was dated to about 200 ka (Readhead, 1984).

Lower Mungo: appearance of freshwater facies over Golgol with well rounded and sorted quartz grains and gravel layers. The Lower Mungo unit is capped by a soil. The soil formation was likely accompanied by carbonate mobilization and a nearly continuous band of cemented sand can be found immediately under the soil horizon. LM3 was buried into the upper part of the Lower Mungo unit. Bowler & Thorne (1976) emphasize that the burial did not contain any material from the Lower Mungo soil. Furthermore, parts of



Figure 1. The LM3 burial (photograph: Alan Thorne).

the skeleton were cemented by carbonates which indicates that the burial took place before the formation of the Lower Mungo soil. Based on correlated radiocarbon data, an age of 28,000 to 30,000 BP was deduced for LM3 (Bowler & Thorne, 1976). A subsequent thermoluminescence dating study (Oyston, 1996) yielded age estimates in the range of about 36 to 50 ka, indicating that the age of the LM3 burial might be well beyond the practical limits of radiocarbon dating of about 40 ka (Chappell *et al.*, 1996a). Recently, Bowler & Price (1998) published a TL date of 41.4 ± 6.7 ka for a sample collected in an equivalent position. Gillespie (1997) inspected the published radiocarbon age determinations from the Lake Mungo area and placed the Lower Mungo/Upper Mungo boundary at about 41,000 cal. BP (Gillespie, personal communication).

Upper Mungo: increasing occurrence of wüstenquartz and gypseous clay pellets indicating increased aridity. The unit contains some minor soil horizons. Originally, the Upper Mungo comprised all sediments between the

Lower Mungo soil and the Zanci Unit. More recently, Bowler (1998) separated the upper sediments of this unit as Arumpo. Oyston (1996) obtained TL dates of 24.6 ± 2.4 (selective bleach) to 34.0 ± 3.9 ka (total bleach) whereas Readhead (1988) obtained TL values of 24.5 ± 3.7 to 29.3 ± 3.2 ka. Gillespie (personal communication) places the Upper Mungo in the range of 38 to 41 cal. BP and Arumpo to between 21,500 to 38,000 cal. BP.

Zanci: mainly gypseous clayey sands, representing the final drying stage of the lake and onset of sustained aridity. Oyston (1996) found TL results of 19.5 ± 2.3 (selective bleach) and 31.6 ± 4 ka (total bleach) and Readhead (1988) obtained 22.3 ± 2.5 ka. Gillespie (personal communication) places the Zanci unit between 18,500 to 21,500 cal. BP.

Note from Figure 2(b) that in some areas of the lunette, these units are not clearly distinguishable. Today, the Walls of China lunette is actively deflating at high rates (up to several centimetres per year). It is not clear whether the deflation was caused by the introduction of cattle and sheep or had started before the white settlement of the area. Nevertheless, the massive deflation, which led to the discovery of the skeletal remains, is a relatively recent process.

In order to better constrain the age of LM3 we have carried out the following dating analyses on the specimen itself:

- mass spectrometric U-series (Th/U) on four bone shavings of LM3;
- gamma spectrometric U-series (Th/U and Pa/U) on the LM3 skull cap;
- ESR on tooth enamel.

Furthermore, we have carried out:

- mass spectrometric U-series (Th/U) on calcitic matrix recovered from the original skeletal material;
- OSL on sediment recovered directly under the lower Mungo soil horizon.

Experimental

Mass spectrometry

The samples analysed were four separate shavings (between 0.17 and 0.28 g) from

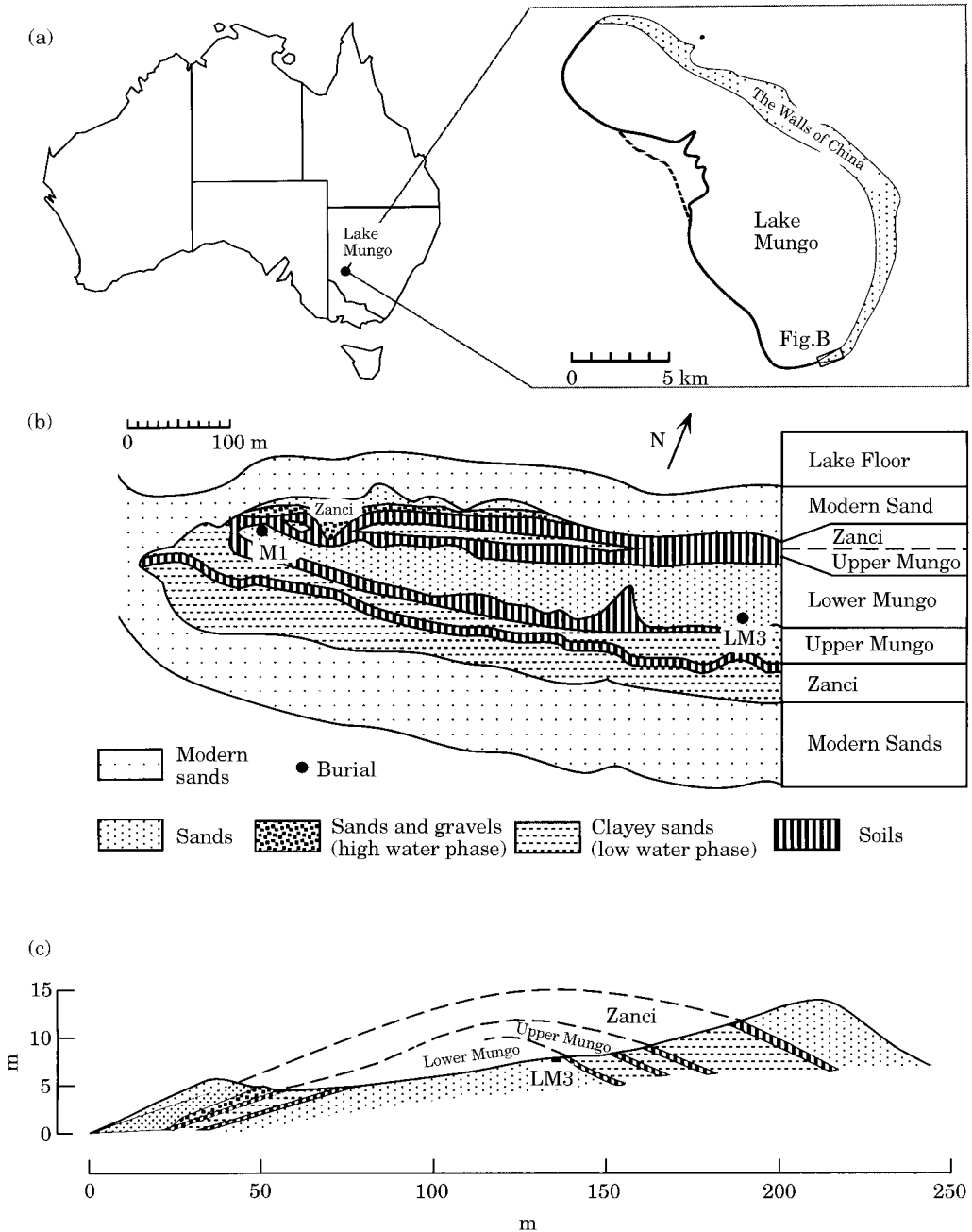


Figure 2. Lake Mungo: geographical position (a), schematic map of the area of the Lake Mungo 3 and 1 burials (b), schematic, composite profile through the lunette (c) (after Bowler & Thorne, 1976).

long bones (samples BA to BD in Table 1) and five samples of a loosely consolidated calcrete-cemented dune sediment (samples SA to SE in Table 1) from the original excavation. The analytical procedures for U-series analyses of faunal material as well as calcitic cement of sediments were recently described by McDermott *et al.* (1996). The calcitic matrix samples were leached with 1 N HNO₃ and any remaining solid matter was centrifuged. The bone samples were completely dissolved in 1 N HNO₃. Both solutions were spiked with "U-2", a mixed ²²⁹Th-²³³U spike, evaporated to a minimum volume of crusty syrup and then dissolved in 2 ml of 7 N HNO₃, ready for ion exchange chemistry. A 2 ml resin bed of Dowex AG-1 X8 200-400# was used for the first stage ion exchange separation. Samples were loaded in 2 ml of 7 N HNO₃, washed three times with 2 ml of 7 N HNO₃, the thorium eluted twice with 2 ml of 8 N HCl and the uranium subsequently eluted three times with 2 ml of 0.5 N HCl. The eluates were taken to dryness, ashed with concentrated HNO₃. The second stage ion exchange separation used separate columns for Th and U, each comprising a 0.15 ml resin bed of Dowex AG-1 X8 200-400#. Samples were re-dissolved and loaded on 0.15 ml of 7 N HNO₃, washed with 3 × 0.15 ml of 7 N HNO₃, and both the thorium and the uranium subsequently eluted three times with 0.25 ml of 0.5 N HCl. The eluates were taken to dryness, ashed with concentrated HNO₃ and set aside to be loaded for mass spectrometry. Total procedural blanks were negligible at <40 pg for ²³²Th and <10 pg for ²³⁸U.

Both Th and U were measured on a MAT 261 thermal ionization mass spectrometer (see Sterling *et al.*, 1995). A double rhenium filament array was used for U and a single rhenium filament for Th. Both were loaded in 1 N HNO₃, the thorium loaded between two thin layers of colloidal graphite. Th data were acquired by sequential peak stepping in an ETP secondary electron multiplier

(SEM) in analogue mode. A typical Th analysis consists of 15 blocks of 10 scans. U data were collected in a combined Faraday cup SEM procedure, where ²³³U, ²³⁵U and ²³⁸U are measured in Faraday cups and ²³⁴U in the SEM. A typical U analysis consists of 15 blocks of 10 scans. Between blocks the relative gain of the SEM over the Faraday cups is measured by placing the ²³⁵U signal in both the SEM and a Faraday cup and comparing the calculated ratios (²³⁵U SEM)/(²³⁸U FAR) and (²³⁵U FAR)/(²³⁸U FAR).

The MAT 261 currently yields ²³⁴U/²³⁵U ratios with a slight negative dependence on the intensity of the ²³⁸U signal. This effect has been calibrated with respect to a secular equilibrium standard uraninite HU-1. Replicate analyses yield the expression: $d^{234}\text{U} = -3.9071 \times (^{238}\text{U volts}) + 4.7819$. The data reported below have been corrected for this offset.

Spike "U-2" has been calibrated for ²²⁹Th/²³³U by measuring a secular equilibrium standard uraninite HU-1, and adjusting the spike Th/U ratio to yield unity for HU-1 [²³⁰Th/²³⁸U]. The absolute ²³⁰Th and ²³⁸U concentrations have been calibrated previously using standard solutions (Sterling *et al.*, 1995). The absolute ²³²Th concentrations are less precisely determined, but in view of the fact that ²³²Th cancels out on isochron plots this is not considered to be a problem.

Gamma spectrometry

Non-destructive gamma spectrometric uranium-series measurements were taken on the partial cranium, which weighs 305 g. The counting system comprises two low background Canberra Packard detectors (see Figure 3). The upper one is an N-type reverse electrode coaxial (CoAx) detector with 40% minimum efficiency. It has a resolution of about 1.05 keV at 122 keV and 1.94 keV at 1332 keV. The detector is capped with 1 mm high purity aluminium

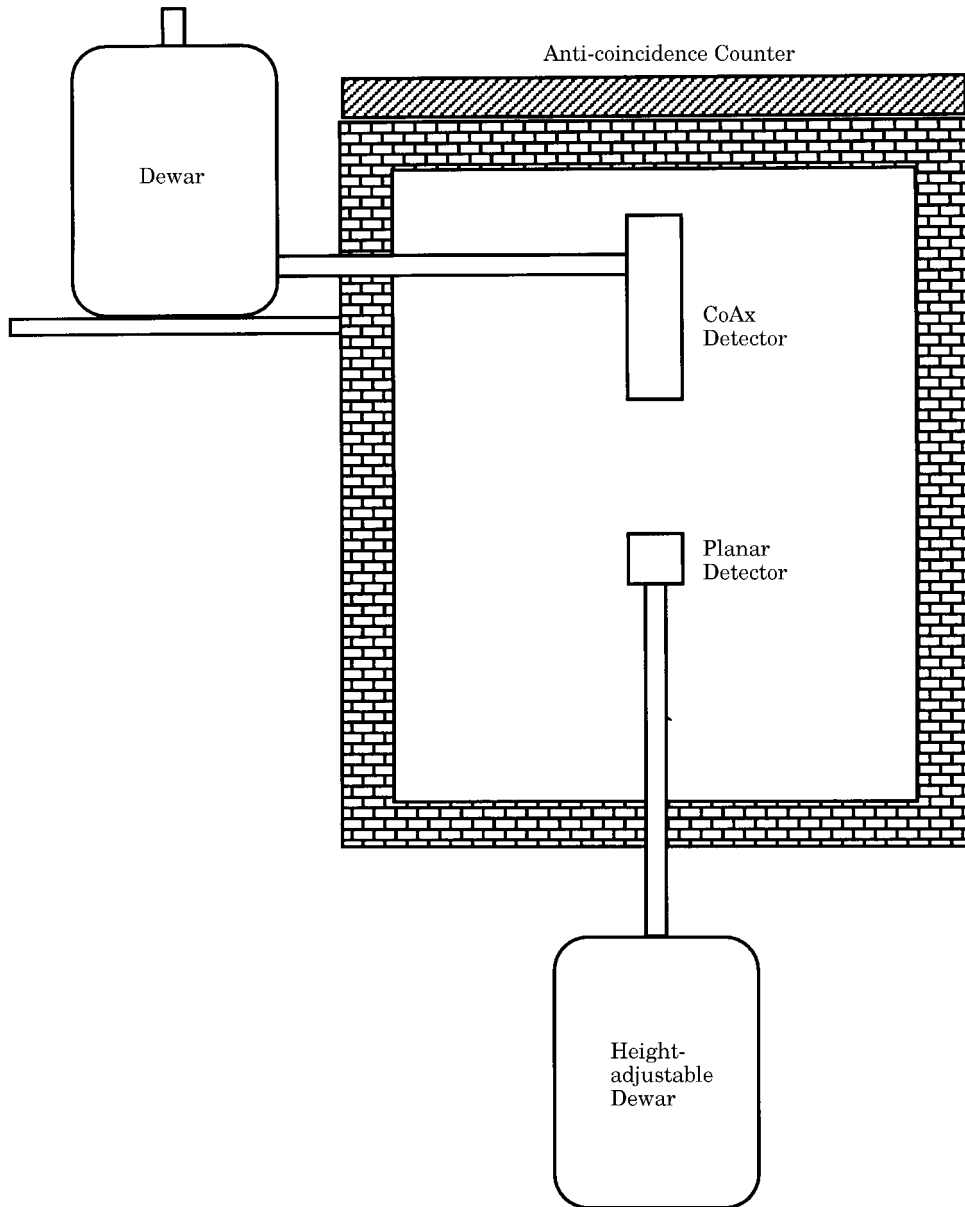


Figure 3. Gamma counting system at ANU (schematic drawing, not to scale). The system comprises a coaxial detector (top) and a planar detector which is height adjustable. This allows the insertion of samples with different sizes and the optimal positioning of both detectors. For minimizing the Rn build-up in the lead shielding, the chamber is flushed with nitrogen. For measurement, the skull is sealed in thick plastic bags and put upside-down on the lower detector so that the co-axial detector is surrounded by the sample for maximum counting efficiency.

which also allows the detection of photons through the side walls. The lower, planar detector has a surface area of 2800 mm² and a thickness of 20 mm. Its resolution is 0.75 keV at 122 keV. Both detectors are cooled with ultra low background cryostats.

The shielding consists of 15 cm lead of which the inner 5 cm were built from selected low activity lead. The cavity is lined with 1 mm tin and 1.5 mm copper foil in order to stop X-rays from the lead. The system is continuously flushed with nitrogen to eliminate any Rn build-up and the plate-out of Rn daughter products in the cavity. The top of the shielding is covered with two plastic detectors which are used as anti-coincidence guards. The background count rates are about 1800 and 4200 counts per hour over the whole energy range for the planar and coaxial detector, respectively. The lower detector assembly is height adjustable so that any sample size (with the largest dimension of <30 cm) can be measured. The samples are placed on the cap of the lower detector and then lifted as close as possible to the upper detector.

In order to avoid surface effects, the cranium was measured for two 50-day periods, being turned over between the measurements. In this study we used a pitchblende doped cast with the same geometry as the cranium as standard, rather than an 80 ppm standard wrapped around a cast which was used in the preliminary study of Simpson & Grün (1998). The isotopes for age calculation were determined via the gamma ray emissions at the following energies: ²³⁸U (²³⁴Th at 63.3 keV); ²³⁰Th (67.7 keV), ²²⁶Ra (186.1 keV, corrected for ²³⁵U at 185.7 keV), ²³⁵U (average of γ -rays at 163.3 and 205.3 keV); ²³¹Pa (via ²²⁷Th at 236.0 keV), ²³²Th (via ²¹²Pb at 238.6 keV).

Electron spin resonance (ESR)

ESR analysis was carried out on a small tooth enamel fragment (10.5 mg) using the single aliquot technique (Grün, 1995)

applying routine laboratory procedures. ESR measurements were carried out on a Bruker ECS 106 spectrometer with a 15 kG magnet and a rectangular 4102 ST cavity. The powdered sample was recorded with the measurement parameters routinely applied in this laboratory: accumulation of 100 scans with 1.015 Gpp modulation amplitude, 10.24 ms conversion factor, 20.48 ms time constant, 2048 bit spectrum resolution (resulting in a total sweep time of 20.972 s), 120 G sweep width and 2 mW microwave power. The sample was irradiated with cumulative doses of 0, 5.5, 10.4, 15.4, 20.4, 30.3, 40.3, 61.1, 102.8, and 180.9 Gy. The past irradiation dose, D_E , and the associated errors, were determined using the procedures outlined by Grün & Brumby (1994). The dose value was obtained from three different approaches: peak-to-peak of the derivative spectra, plateau of the integrated spectra (Grün & Jonas, 1996) as well as spectrum deconvolution (Grün, 1998). The average dose obtained from the three methods is 26 ± 2 Gy.

U and Th of the dental material and adhering sediment were determined by ICP-MS (Grün & Taylor, 1996), and K of the sediment by flame photometry. The following data were used for ESR age calculation: dentine 3.82 ± 0.19 ppm U, $2.5 \pm 1.25\%$ water; enamel 0.35 ± 0.02 ppm U; α -efficiency 0.13 ± 0.02 (Grün & Katzenberger-Apel, 1994); enamel thickness 500 ± 200 μ m, beta attenuation using Monte-Carlo attenuation factors as published by Brennan *et al.* (1997) and experimentally confirmed by Yang (1997); sediment: 0.27 ± 0.05 ppm U, 0.82 ± 0.04 ppm Th, $0.15 \pm 0.01\%$ K, $2.5 \pm 1.25\%$ water. The sediment data were used for external beta dose rate (39 ± 8 μ Gy/a). The gamma dose rate (90 ± 6 μ Gy/a) is an average of *in situ* measurements of the upper part of the Lower Mungo unit. The cosmic dose rate (139 ± 10 μ Gy/a) was calculated for

rapid deposition of 1 m Lower Mungo, soil development for 21 ka without erosion or sedimentation, constant deposition of 3 m Upper Mungo between 41 and 22 ka, constant deposition of 3 m Zanci during 22 to 19 ka, with no further sedimentation after that and final erosion during the last 200 years. The error in the cosmic dose rate accounts for alternative sedimentation models. Note that longtime variations of the cosmic dose rate at the Earth's surface are negligible (Prescott & Hutton, 1994).

We also considered $64 \pm 3\%$ Rn loss from dentine as measured by gamma spectrometry on Mungo 3 skull, using the intensities of ^{230}Th at 67.7 keV and ^{210}Pb at 46.5 keV. ESR ages were calculated for closed system, early U-uptake (EU), and continuous, linear U-uptake (LU). For more details on ESR dating, see Grün (1989).

Optically stimulated luminescence (OSL)

Optical dating (Huntley *et al.*, 1985; Aitken, 1994, 1998) is a luminescence dating technique capable of providing numerical ages for sediment, the event dated being the last exposure to sunlight. The technique relies on measurement of optically stimulated luminescence (OSL) emitted by minerals such as quartz under illumination by visible light, and so is well suited to the dating of unburnt sediment. One of us (N.A.S.) has applied the method to sediments collected from the Lower Mungo unit in the course of a joint study between scientists and the three traditional tribal groups in the Willandra Lakes region, and funded by the Australian Institute of Aboriginal and Torres Strait Islander Studies (AIATSIS) with a grant to Professor I. McBride. The optical dates presented here are part of that study and the full details will appear in Spooner *et al.* (in preparation).

Two sediment samples were collected using steel coring tubes within the Lower Mungo unit 30 cm below the carbonate

horizon of the Lower Mungo soil, at a level stratigraphically equivalent to the burial depth of LM3. Quartz grains of 90–125 μm were subsequently extracted under low-intensity red light in the laboratory by a procedure including HCl acid digestion, sieving, heavy liquid flotation, and finally etching in 48% HF acid etching for 40 min to remove the outer 6–8 μm alpha-particle irradiated shell, then loaded on to stainless steel discs.

All OSL measurements for dose determination were undertaken using an Elsec Type 9010 automated reader and Type 9022 beta irradiator. Multiple-aliquot additive and multiple-aliquot regenerative dose-response curves were each constructed using 64 aliquots and subsequently combined for dose determination using the "Australian Slide" method (Prescott *et al.*, 1993). The measurement procedure involved initial recording of the natural OSL during a 0.1 s illumination for normalization, prior to laboratory irradiation. Irradiation was then administered from a $^{90}\text{Sr}/^{90}\text{Y}$ beta plaque at a dose rate of 2.74 ± 0.08 Gy/min following which all aliquots received simultaneous preheating at 220°C for 300 s. OSL emitted from each aliquot during 300 s illumination by 500 ± 40 nm light was detected by an EMI 9235Q bi-alkali photomultiplier tube optically filtered by 2.5 mm U-340 and 3 mm Schott UG 11 colour glass filters.

The assessment of the dose rate from the sediments presented specific difficulties, on account of low radioisotope activity and the containment of a large proportion of this activity within the quartz grains themselves, giving rise to small-scale heterogeneity of distribution. The low radioisotope concentration in the Lower Mungo sediments site also had the consequence that cosmic rays contribute a significant component of the total dose rate. This contribution was estimated by means of palaeo-stratigraphic reconstruction to determine burial depths and durations, in a manner similar to

Oyston (1996). The dose rates at the various burial depths were calculated from Prescott & Hutton (1994). *In situ* water content was measured, and the saturation capacity deduced from the calculated sediment porosity.

K was measured for the bulk sediment using NAA/DNA, XRF and high resolution γ -spectrometry and for the HF-etched quartz fraction using XRF. U and Th were measured in the etched quartz by INAA, NAA/DNA and ICPMS, and the U and Th decay chains by α -spectrometry. U and Th concentrations in the bulk sediment were measured by INAA, NAA/DNA and ICPMS, and the decay chains by α -spectrometry and γ -spectrometry. For age calculation the means of all analyses were used.

The α -efficiency was measured using a Risø TL-DA-8 reader with 420–560 nm stimulation and emissions detected through two 3 mm U-340 filters. The α -efficiency (a -value) was found to be between 0.043 and 0.036. This value is substantially lower than that found by Oyston (1996) for TL production in this unit, but closely agrees with previously found a -values for OSL and IRSL on quartz from sediments (Questiaux, 1990; Rees-Jones & Tite, 1997). The Lower Mungo sediment was deduced from the α -spectroscopy data to be in secular equilibrium.

Ages were calculated using the *AGE2* program of R. Grün which is based on dose rates by Adamiec & Aitken (1998). A modern age was found for a surface sample, confirming the efficacy of solar resetting of the optical dating signal, at least in the contemporary environment.

Results

The U-series and ESR age estimates are summarized in Table 1. It is clear that all results are consistently older than 40,000

years, the practical limit of radiocarbon dating.

Mass spectrometric U-series dating

Bones and teeth are open systems for uranium and by far the dominant process is uranium uptake (e.g., Grün & McDermott, 1994; Grün *et al.*, 1999). Therefore, closed system ESR and U-series results on faunal material are usually regarded as minimum age estimates. However, there are also cases where U-loss has been observed (e.g., Chen & Yuan, 1988). The occurrence of calcitic matrix in the sediment immediately adhering to the human bones, as well as directly on the bones, indicates that the calcitic precipitation took place after the burial of the bones. Thus, the calcitic precipitations provide only minimum age estimates for the bones.

Figure 4(a) shows the mass spectrometric results on the bone samples. Given the undisputed contemporaneity of the samples, the range in the mass spectrometric Th/U ages clearly displays the effect of uranium mobilization. The samples with the higher U-concentrations (samples BC, BD) have lower apparent U-series ages than those with lower U-concentrations (BA, BB). The sequence of ages can be explained by both delayed U-uptake and recent U-loss. On the one hand, the bones may have experienced a relatively fast uptake of about 3 to 3.5 ppm of uranium at about 70 ka ago, samples BB, BC and BD continued to accumulate uranium up to about 5.5 ppm, thus yielding apparently younger U-series ages than sample BA. Of course, all samples may have experienced delayed U-uptake and the correct age of LM3 is older than 70 ka. On the other hand, all samples may have accumulated about 5.5 ppm uranium about 50 ka ago and, along with the relatively recent deflation of the lunette, uranium was oxidized and removed from the bones. The more uranium is lost from the bones, the older become their apparent U-series ages.

Table 1 Isotopic values of U-series analyses (for comparison, isotopic ratios are given as activity ratios and all uncertainties are 1- σ)

	U (ppm)	$^{234}\text{U}/^{238}\text{U}$	$^{230}\text{Th}/^{238}\text{U}$	$^{230}\text{Th}/^{234}\text{U}$	$^{230}\text{Th}/^{232}\text{Th}$	$^{226}\text{Ra}/^{230}\text{Th}$	Th/U Age (ka)	$^{231}\text{Pa}/^{235}\text{U}$	Pa/U Age (ka)	ESR Age (ka)
Mass spectrometry										
Bone										
BA	3.574 ± 0.022	1.369 ± 0.002	0.6651 ± 0.0144		22.3 ± 0.5		69.8 ± 2.1			
BB	3.889 ± 0.022	1.358 ± 0.001	0.5754 ± 0.0087		21.1 ± 0.4		58.3 ± 1.2			
BC	5.613 ± 0.022	1.354 ± 0.001	0.5143 ± 0.0075		21.2 ± 0.4		50.7 ± 0.9			
BD	5.445 ± 0.022	1.362 ± 0.002	0.5478 ± 0.0052		21.9 ± 0.3		54.5 ± 0.7			
Sediment										
SA	0.244	1.330 ± 0.003		0.615 ± 0.051	2.93 ± 0.25					
SB	0.232	1.341 ± 0.002		0.744 ± 0.063	2.84 ± 0.24					
SC	0.242	1.343 ± 0.004		0.745 ± 0.075	3.87 ± 0.39					
SD	0.076	1.322 ± 0.003		1.127 ± 0.195	1.77 ± 0.30					
SE	0.277	1.189 ± 0.006		0.843 ± 0.117	1.39 ± 0.19					
Isochron		1.343 ± 0.085		0.542 ± 0.097			82 ± 21			
Gamma spectrometry										
Planar										
A	8.8		0.62 ± 0.05		22.9 ± 3.3	0.81 ± 0.07		0.77 ± 0.08		
B			0.59 ± 0.05		15.9 ± 2.1	0.83 ± 0.07		0.73 ± 0.06		
CoAx										
A	5.9		0.74 ± 0.04		18.4 ± 1.6	0.72 ± 0.04		0.78 ± 0.05		
B			0.63 ± 0.05		12.4 ± 2.0	0.91 ± 0.07		0.88 ± 0.06		
Weighted mean										
		1.361 ± 0.006*	0.66 ± 0.02		16.7 ± 1.0	0.78 ± 0.03	69.5 ± 2.9*	0.79 ± 0.03	74 ± 7	
		1.319 ± 0.035†	0.60 ± 0.02‡				64.1 ± 3.7‡	0.72 ± 0.03‡	60 ± 5‡	
ESR										
										63 ± 6 (EU)
										78 ± 7 (LU)

*Using the average mass-spectrometric $^{234}\text{U}/^{238}\text{U}$ ratio of the four bone shavings BA to BD.

†Using the mass-spectrometric $^{234}\text{U}/^{238}\text{U}$ ratio from Figure 4(b) and an initial $^{230}\text{Th}/^{232}\text{Th}$ of 1.5.

‡Using an initial $^{231}\text{Pa}/^{235}\text{U}$ ratio of 0.046.

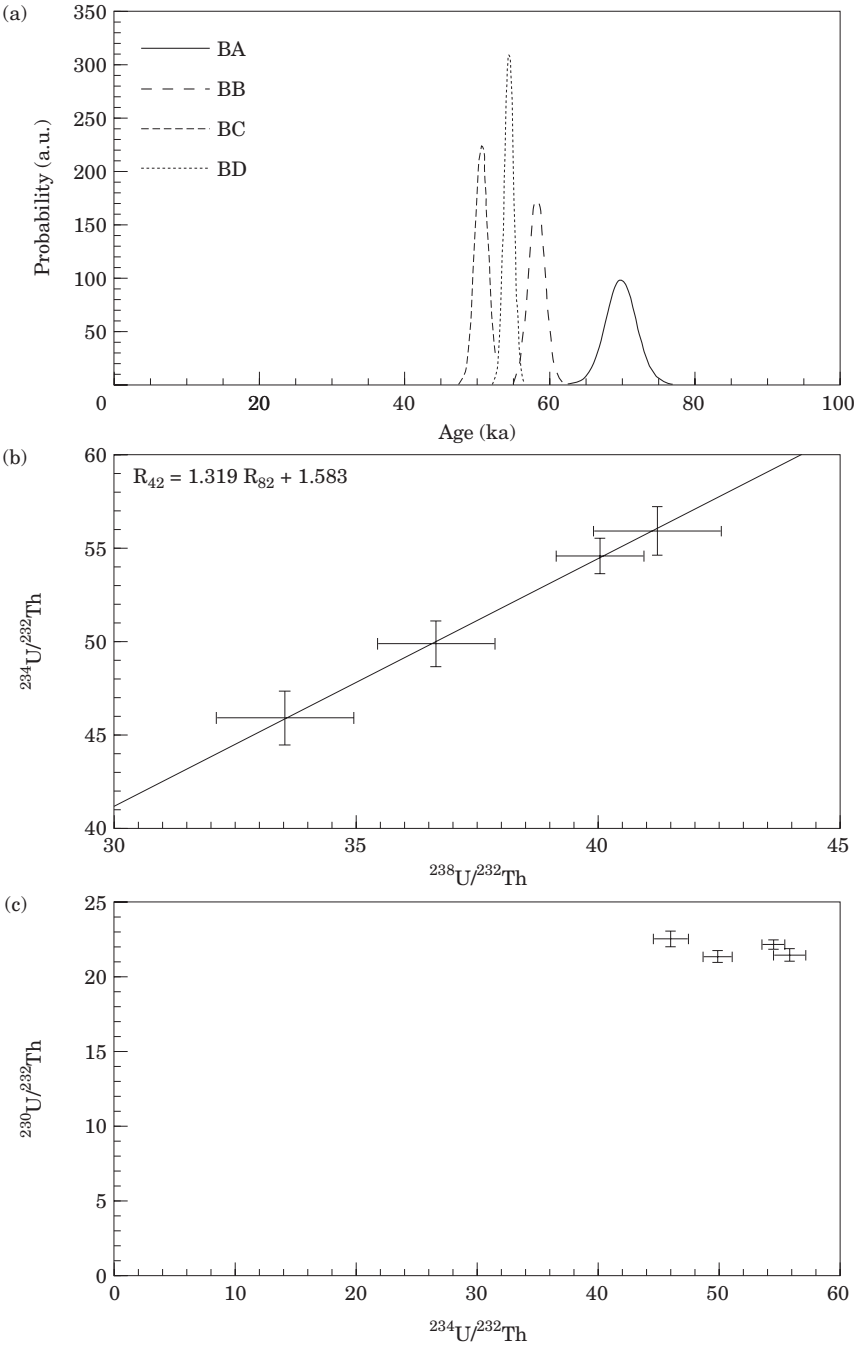


Figure 4. Mass spectrometric U-series results on the four bone shavings (a). The scatter of the apparent ages is due to uranium mobilization. The $^{234}\text{U}/^{232}\text{Th}$ ($=R_{42}$) vs. $^{238}\text{U}/^{232}\text{Th}$ ($=R_{82}$) plot (b) shows that the $^{234}\text{U}/^{238}\text{U}$ ratio in the different samples was not altered by U-mobilization. It can therefore be assumed that the same $^{234}\text{U}/^{238}\text{U}$ ratio is found in other parts of the skeleton. The plot of $^{230}\text{Th}/^{232}\text{Th}$ vs. $^{234}\text{U}/^{232}\text{Th}$ (c) does not result in an isochron.

Again, all subsamples may have experienced recent U-loss and the correct age of the sample may be younger than 50 ka.

The $^{234}\text{U}/^{232}\text{Th}$ versus $^{238}\text{U}/^{232}\text{Th}$ plot [Figure 4(b)] shows that the $^{234}\text{U}/^{238}\text{U}$ ratio in the four bone samples was not affected by uranium mobilization. If uranium was accumulated over longer time ranges, the source composition of the uranium did not change. If uranium was leached recently, ^{234}U was not preferentially removed. The close agreement of the $^{234}\text{U}/^{238}\text{U}$ ratios of the four bone samples imply that the same $^{234}\text{U}/^{238}\text{U}$ ratio can also be found in the other parts of the skeleton, e.g., the skull. Not surprisingly, the $^{230}\text{Th}/^{232}\text{Th}$ versus $^{234}\text{U}/^{232}\text{Th}$ plot [Figure 4(c)] does not result in a meaningful fit. All bone samples show some detrital ^{232}Th with $^{230}\text{Th}/^{232}\text{Th}$ ratios close to 22. Unfortunately, the isochron data cannot be used to estimate an initial $^{230}\text{Th}/^{232}\text{Th}$ ratio. If we assume that the initial $^{230}\text{Th}/^{232}\text{Th}$ ratio is in the range of 1 to 1.5 [as often assumed in U-series studies of speleothems (e.g., Schwarcz, 1980)], the U-series results would become younger by about 5 to 7%.

To summarize, the mass spectrometric U-series data on the bones show that the four different bone samples have closely agreeing $^{234}\text{U}/^{238}\text{U}$ ratios, but their apparent ages range from 50 to 70 ka. This age range may reflect different histories of U-mobilization such as delayed U-uptake, recent U-loss or a combination of these processes. The mass spectrometric data alone do not enable us to distinguish between these two uranium mobilization processes.

Figure 5(a) and (b) show the isochron plots of the mass spectrometric U-series data on the calcitic fraction of the matrix. The fitted $^{230}\text{Th}/^{234}\text{U}$ and $^{234}\text{U}/^{238}\text{U}$ values result in an isochron age of 81 ± 21 ka using the *Isoplot* program of K. Ludwig for data fitting and age calculation (see Ludwig & Titterton, 1994). The large uncertainty in the age estimate is caused by the low

U-concentrations and consequently low ^{230}Th count rates, as well as the relatively small spread in the $^{230}\text{Th}/^{232}\text{Th}$ isotope ratios. We note that the isochron $^{234}\text{U}/^{238}\text{U}$ ratios of the bone and the soil samples agree within error. This may be taken as an indication that the source of the uranium in carbonate and bone was the same and that uranium migrated into the bones at the same time as the carbonate was precipitated.

U-series dating: gamma spectrometry

Because of inherently large uncertainty in the gamma spectrometric measurement of $^{234}\text{U}/^{238}\text{U}$ ratios [Simpson & Grün (1998) calculated a value of 1.62 ± 0.87], we have used the average mass spectrometric value of the uniform $^{234}\text{U}/^{238}\text{U}$ ratio of the bone shavings (samples BA to BD) to calculate $^{230}\text{Th}/^{234}\text{U}$ ages. Table 1 shows that the dating results using the mean Pa/U and Th/U isotopic ratios are very close. Note that the gamma spectrometric values of Table 1 are slightly different to those published by Simpson & Grün (1998), who used a different standard and means that were based on a single 50-day measurement period. All bone samples contain significant amounts of ^{232}Th . This implies that the bone samples also accumulated some amount of unsupported, detrital ^{230}Th (see, e.g., Schwarcz, 1980, 1997). Age calculations and modelling has been carried out for initial $^{230}\text{Th}/^{232}\text{Th}$ ratios of 0 and 1.5.

Initial $^{230}\text{Th}/^{232}\text{Th} = 0$

The Th/U and Pa/U age estimates can now be used to ascertain whether uranium uptake or loss has occurred. Figure 6 shows the concordance diagrams where the mean gamma spectrometric $^{231}\text{Pa}/^{235}\text{U}$ ratio is plotted against the mean $^{230}\text{Th}/^{238}\text{U}$ ratio. Concordance between the two ratios is obtained for early U-uptake (i.e., both ratios yield the same age) if the $^{234}\text{U}/^{238}\text{U}$ ratio is in the range of about 1.31 ± 0.09 [Figure 6(a)]. For linear U-uptake, concordance is

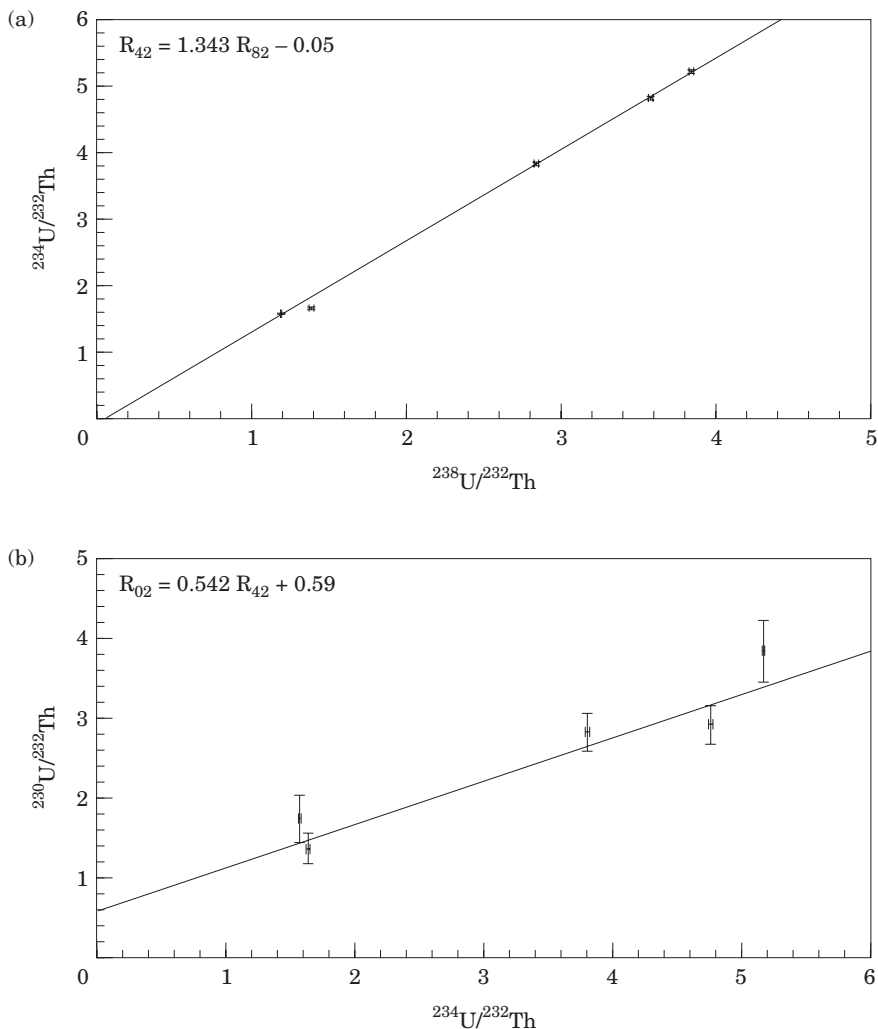


Figure 5. Mass spectrometric U-series results on the five sediment leachates (i.e., the carbonate precipitations on the bones). (a) The $^{234}\text{U}/^{232}\text{Th}$ ($=R_{42}$) vs. $^{238}\text{U}/^{232}\text{Th}$ ($=R_{82}$) plot shows that the $^{234}\text{U}/^{238}\text{U}$ ratio is very similar to the value obtained on the bones [see Figure 4(b)]. This may be taken as an indication that the uranium source for the bones and carbonate precipitation was the same. (b) The plot of $^{230}\text{Th}/^{232}\text{Th}$ ($=R_{02}$) vs. $^{234}\text{U}/^{232}\text{Th}$ in combination with the $^{234}\text{U}/^{238}\text{U}$ ratio (above) yield an age of 82 ± 21 ka.

achieved if the $^{234}\text{U}/^{238}\text{U}$ ratio is in the range of 1.13 ± 0.09 [Figure 6(b)]. The measured mass spectrometric $^{234}\text{U}/^{238}\text{U}$ ratio of 1.361 ± 0.006 [thick, dotted line in Figure 6(a, b)] shows that the LU model is not appropriate for the calculation of U-series ages. Instead, an offset to the opposite direction is observed. This might have

been caused by recent U-loss [see Figure 6(c)]. The offset of the measured $^{234}\text{U}/^{238}\text{U}$ ratio from the expected EU concordance value corresponds to recent U-leaching in the range of 7% (in which case the measured gamma spectrometric Pa/U and Th/U ratios are concordant with the measured mass spectrometric $^{234}\text{U}/^{238}\text{U}$ ratio). If such a

small amount of modern leaching has occurred, the U-series age is reduced to 63 ± 6 ka.

The gamma spectrometric measurements can also be used for assessing Ra mobilization via the γ -ray peak at 186 keV which consists of γ -ray emission from ^{226}Ra and ^{235}U (see $^{226}\text{Ra}/^{230}\text{Th}$ ratios in Table 1). The averaged $^{226}\text{Ra}/^{230}\text{Th}$ ratio of 0.78 ± 0.03 implies that the sample has experienced a relatively recent Ra loss of at least $22 \pm 3\%$ (any Ra mobilization prior to 10 ka is not measurable due to the relative short half life of ^{226}Ra of 1600 years). LM3 is so far the only sample for which we measured any notable Ra mobilization and gives an indication that the bones of LM3 were geochemically activated in recent times. It is most likely that the Ra mobilization coincides with the recent denudation of the dunes. Considering that Ra is far more mobile than U (see, e.g., Longtin, 1988; Osmond & Ivanovich, 1992), any U mobilization should be on a smaller scale.

Initial $^{230}\text{Th}/^{232}\text{Th} = 1.5$

When correcting U-series ages for detrital, unsupported ^{230}Th , the Th/U ages become younger. If we assume an initial ratio of 1.5 and using the mass spectrometric $^{234}\text{U}/^{238}\text{U}$ ratio of 1.319 ± 0.035 [from Figure 4(b), this ratio accounts for detrital Th], we obtain a closed system Th/U age of 64.1 ± 3.7 ka, which is about 8% younger than the uncorrected value (see Table 1). It is reasonable to assume that the samples also contained detrital Pa with an initial $^{231}\text{Pa}/^{230}\text{Th}$ ratio close to 0.046 which is the natural activity ratio of $^{235}\text{U}/^{238}\text{U}$. We note that the closed system Th/U, and Pa/U age estimates, corrected for detrital Th and Pa, agree within errors. When plotting the corrected $^{230}\text{Th}/^{238}\text{U}$ and $^{231}\text{Pa}/^{235}\text{U}$ ratios in the concordance diagrams (Figure 7), we observe that the data point lies above the mass spectrometric $^{234}\text{U}/^{238}\text{U}$ ratio of 1.319 in the EU concordance plot and below in

the LU plot. This implies delayed U-uptake. The Th/U and Pa/U age estimates converge for a P -value of -0.72 (using the open system notation of Grün *et al.* (1988) where $P=1$ corresponds to the closed system EU age and $P=0$ to linear U-uptake), corresponding to an age estimate of about 86 ka.

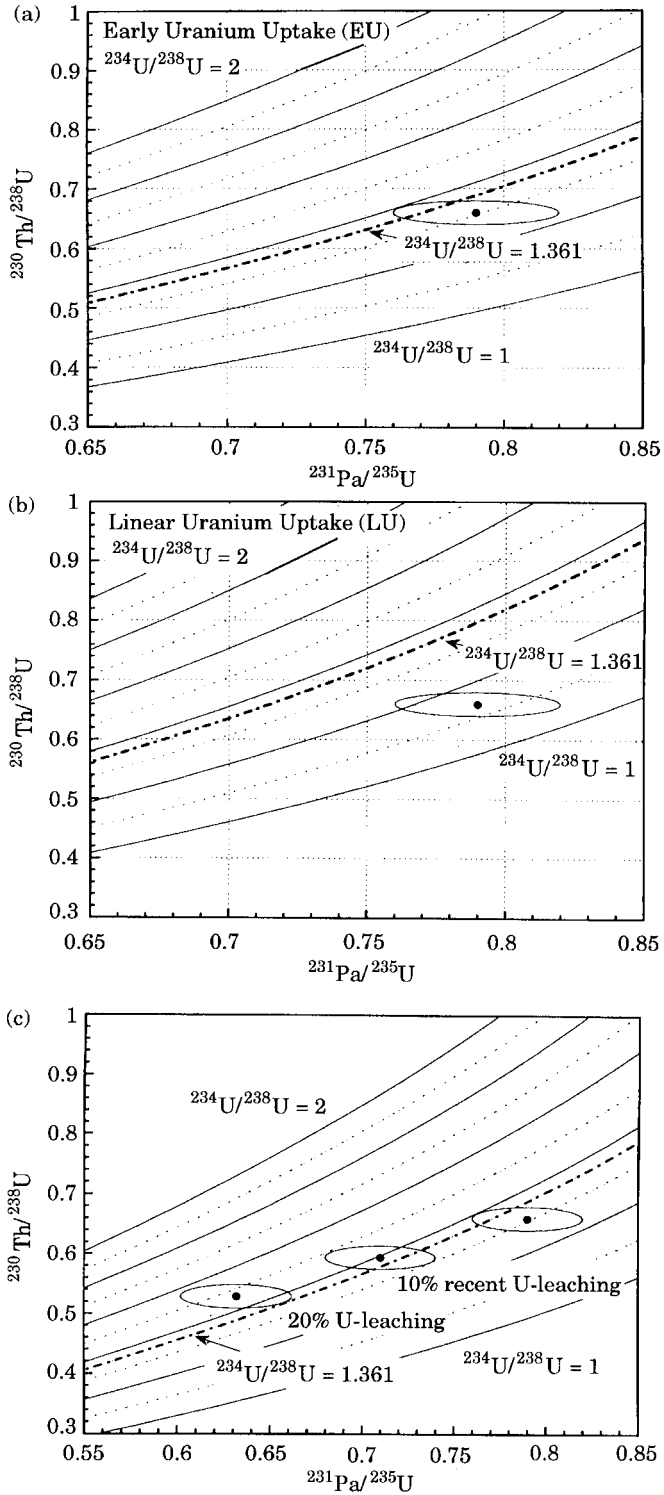
ESR dating

Calculated dose rates are (in $\mu\text{Gy/a}$): external beta from sediment: 39 ± 8 ; external beta from dentine: 59 ± 10 (EU); 29 ± 5 (LU); internal: 84 ± 10 (EU); 38 ± 6 (LU). ESR dating yielded a closed system age estimate of $63,000 \pm 6000$ years (EU) and an open system age of $78,000 \pm 7000$ years (LU) (see Table 1). The calculated 64% Rn loss has an overall effect of 2.5 ka (EU) and 1 ka (LU) on ESR age calculation.

Combination of ESR and U-series age estimates

The components of the tooth (dentine, enamel) should have experienced similar U mobilization to the skull. In order to assess the possible effect of U-mobilization, U-series and ESR results are combined. Provided that U-series and ESR calculations are governed by the same process (U-leaching if no detrital Th correction is carried out; U-uptake if a detrital Th correction is carried out), U-series and ESR age estimates should converge for the appropriate open system model. Considering the mathematical complexity of open system modelling for combining U-series and ESR age estimates (see Grün *et al.*, 1988), we have carried out stepwise calculation separately for each dating method and use the error of the mean as convergence criterion (similar procedures have basically applied for any iterative calculation).

Initial $^{230}\text{Th}/^{232}\text{Th} = 0$. Figure 8(a) shows the mean and standard deviation (expressed as percentage error of the mean) of the Th/U, Pa/U and ESR age estimates for a variety of



recent U-losses. The age estimates converge for a recent U-loss of 7.5% (corresponding to a mean age of 62.1 ± 0.6 ka). The individual errors of the modelled Th/U, Pa/U and ESR age estimates overlap in the range of 0 to 15% U-loss, corresponding to a mean age range of between 56 and 68 ka.

Initial $^{230}\text{Th}/^{232}\text{Th}=1.5$. Figure 8(b) shows the mean and standard deviation of the Th/U, Pa/U and ESR age estimates for a variety of U-uptake histories. The age estimates converge for the closed system age (corresponding to a mean age of 62.4 ± 2.0 ka). The individual errors of the modelled Th/U, Pa/U and ESR age estimates overlap in the range of $P=-1$ to $P=-0.9$, corresponding to a mean age range of between 62 and 69 ka.

Surprisingly, the different scenarios give very robust age estimates for the skeletal remains. This lies in the fact, that the ESR age estimate is significantly less influenced by U-mobilization than the U-series results.

OSL dating

The details of the OSL results are listed in Table 2. The OSL age estimates of the two samples, 59 ± 3 and 63 ± 4 ka, result in a weighted mean of 61 ± 2 ka. This age estimate should in principle provide a maximum age for the LM3 specimen because the deposition of the sediment took place before the burial of the skeleton.

Discussion

Considering the uncertainties of the individual measurements, the mean age of LM3 skeletal remains, combining ESR and U-series, is 62 ± 6 ka.

The U-series results imply that some uranium mobilization has taken place. The measured $^{226}\text{Ra}/^{230}\text{Th}$ ratios indicate recent geochemical activation of the bones which is most likely associated with the recent deflation of the lunette. With respect to open system modelling, it may well be that the actual U-history of the skull was somewhat different from the components of the tooth, that the initial, detrital $^{230}\text{Th}/^{232}\text{Th}$ and $^{231}\text{Pa}/^{230}\text{Th}$ ratios were different than those considered above, and that some delayed U-uptake has taken place shortly after the tooth was buried. Different U-mobilization histories may add some additional uncertainty to the age estimates. At present we do not have any further evidence that can be used for alternative modelling. We would find it difficult, however, to invent explanations that could accommodate combined U-series/ESR ages of less than 50 ka.

The OSL result of this study, 61 ± 2 ka, are consistent with four other OSL dates from the Lower Mungo unit (Spooner *et al.*, in preparation) as well as all of the other age estimates of this study. However, it is considerably older than the single TL date of Oyston (1996) who reported an age of between 36 and 50 ka for his sample J3 which is most closely associated with LM3. The difference between the data sets lies in the dose determination. We notice from

Figure 6. No correction for detrital ^{230}Th and ^{231}Pa . $^{231}\text{Pa}/^{235}\text{U}$ and $^{230}\text{Th}/^{238}\text{U}$ concordance diagrams for early U-uptake (a) and linear uranium uptake (b) using mean gamma spectrometric values. Concordance is achieved when the measured $^{231}\text{Pa}/^{235}\text{U}$ and $^{230}\text{Th}/^{238}\text{U}$ ratios give the same age result. The appropriate $^{234}\text{U}/^{238}\text{U}$ ratio is obtained from the iso- $^{234}\text{U}/^{238}\text{U}$ lines: 1.31 ± 0.09 for early U-uptake (=closed system) and 1.13 ± 0.09 for linear U-uptake. The average mass spectrometric $^{234}\text{U}/^{238}\text{U}$ ratio of 1.361 ± 0.006 (thick dotted line) shows that the gamma spectrometric results are close to the early U-uptake model. If recent U-leaching has taken place (which may be indicated by the fact that the EU $^{234}\text{U}/^{238}\text{U}$ concordance ratio is smaller than the measured $^{234}\text{U}/^{238}\text{U}$ ratio), it would be in the range of 7% (c).

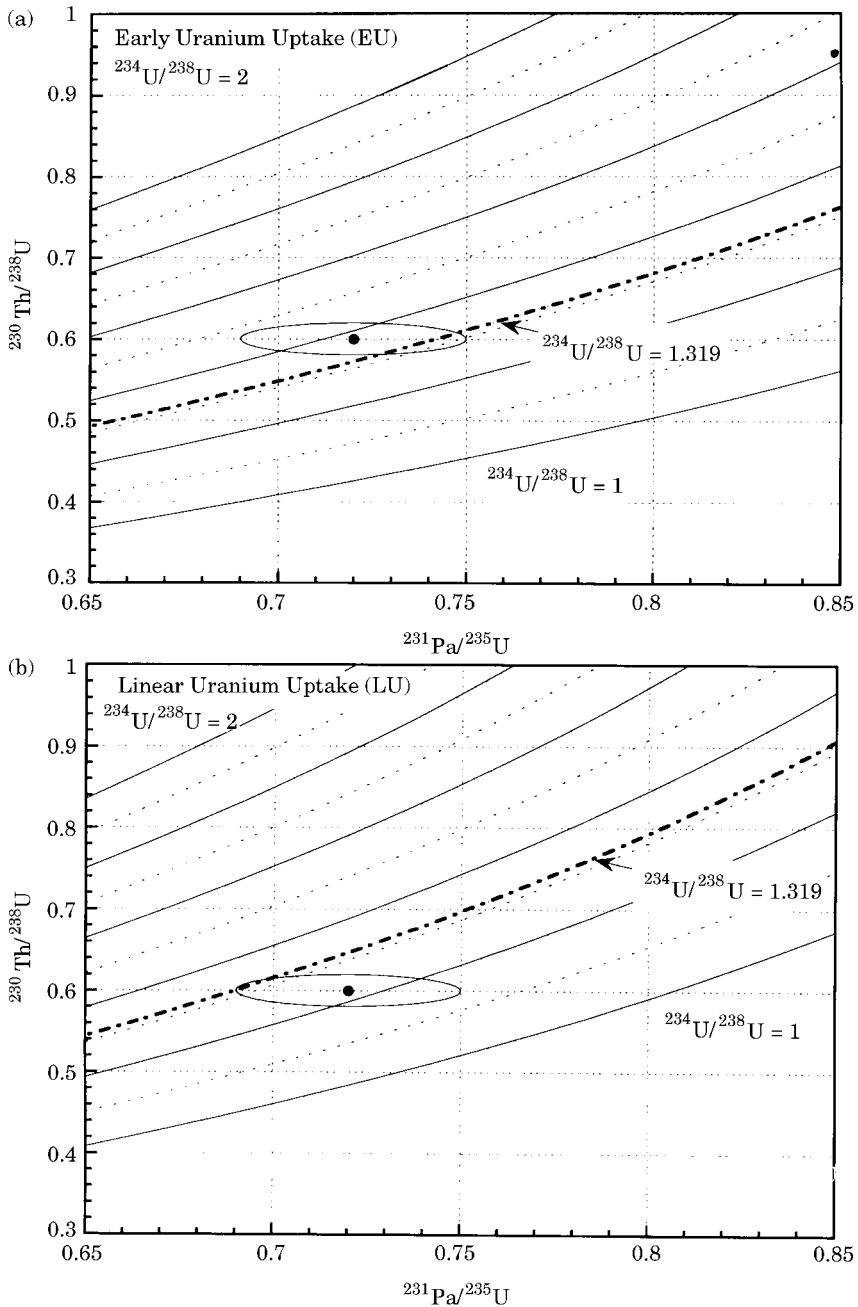


Figure 7. Correction for detrital ^{230}Th ; initial $^{230}\text{Th}/^{232}\text{Th} = 1.5$. Concordance diagrams for early U-uptake (a) and linear uranium uptake (b) using mean gamma spectrometric values corrected for detrital ^{230}Th and ^{231}Pa . The Th corrected average mass spectrometric $^{234}\text{U}/^{238}\text{U}$ ratio of 1.319 ± 0.006 [thick dotted line, this value is obtained from Figure 4(b)] shows that the gamma spectrometric results are between the EU and LU models; i.e., implying U-uptake. Concordance with the mass spectrometric $^{234}\text{U}/^{238}\text{U}$ ratio is obtained for a P -value of -0.72 (for P -value notation see Grün *et al.*, 1988, where $P = -1$ corresponds to the closed system EU age and $P = 0$ to linear U-uptake) resulting in a mean value of about 86 ka.

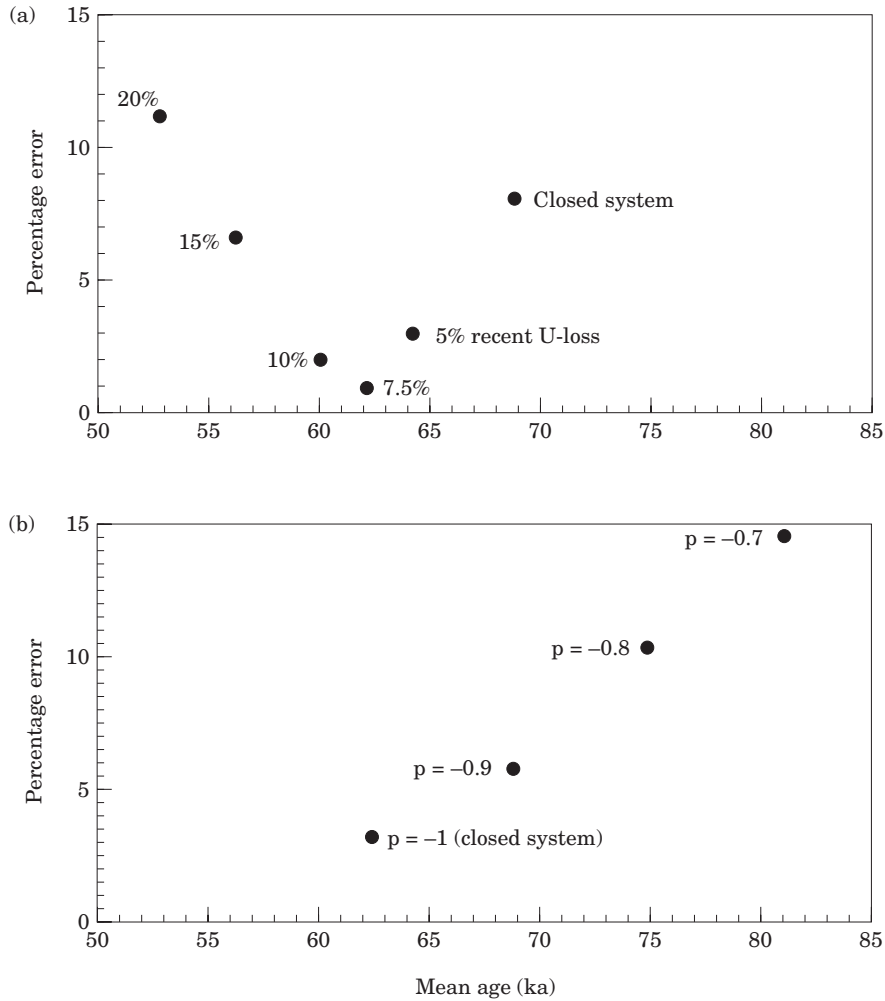


Figure 8. Combination of U-series and ESR age results. Provided that uranium mobilization in the components of the tooth as well as in the bones is governed by the same process (U-leaching if no detrital Th correction is carried out or U-uptake if a detrital Th correction is carried out), U-series and ESR age estimates should converge for the appropriate open system model. When no correction for detrital ^{230}Th is carried out (a), ESR, Th/U and Pa/U age estimates converge at 62.1 ± 0.6 ka (which is expressed by the smallest error in the mean value). If this model is correct, some minor recent leaching of uranium (7.5%) would have taken place. When correcting for detrital ^{230}Th and ^{231}Pa components (b), ESR, Th/U and Pa/U age estimates converge at 62.4 ± 2 ka, which is the closed system age.

Figure 7 in Oyston (1996) that sample J3 must have had a much higher sensitivity to dose than the other samples in that study (the natural intensity of J3 is about double of J1, but the dose of J3 is smaller than that of J1). However, the radiation sensitivity of the samples from the Mungo dune, including

those related to LM3, analysed by Spooner (unpublished data), does not significantly change. This anomalous sensitivity of sample J3 may explain its apparent age underestimation. The TL date by Bowler & Price (1998) shows a similar dose value (24.7 ± 3.4 Gy) as obtained in this study,

Table 2 Results of OSL analysis

Sample	D_E (Gy)	int. U (ppm)	int. Th (ppm)	α -efficiency	ext. U (ppm)	ext. Th (ppm)	ext. K (%)	Water (%)	cosmic \dot{D} (μ Gy/a)	int. \dot{D} (μ Gy/a)	ext. \dot{D} (μ Gy/a)	total \dot{D} (μ Gy/a)	Age (ka)
ANU _{OD} 174a	23.6 ± 0.6	0.07 ± 0.03	0.25 ± 0.05	0.044 ± 0.010	0.22 ± 0.01	1.01 ± 0.08	0.11 ± 0.01	2.5 ± 0.8	139 ± 10	21 ± 4	237 ± 8	397 ± 16	59 ± 3
ANU _{OD} 174d	25.5 ± 0.5	0.10 ± 0.01	0.29 ± 0.06	0.036 ± 0.010	0.26 ± 0.01	1.16 ± 0.02	0.10 ± 0.01	2.5 ± 0.8	139 ± 10	24 ± 5	239 ± 8	402 ± 16	63 ± 3

but their dose rate estimates are considerably higher. The differences between the estimated dose and dose rate values between the luminescence studies may imply that the samples were not collected from comparable positions. We note that neither Oyston (1996) nor Bowler & Price (1998) went to the same length as this study for the precise estimation of dose (derived from the measurement of 128 disks) and dose rate (each elemental value was determined through repeated runs using at least three independent analytical techniques).

It is worth mentioning that the stratigraphic relationship between the hearth sites in the "Walls of China" lunette on which various TL studies were carried out (e.g., Huxtable & Aitken, 1977; Readhead, 1988; Bell, 1991), situated between 5 and 7 km north of the LM3 burial, and the LM3 burial is problematic (Bowler, 1998; Magee, personal communication).

The age result on the human skeleton, 62 ± 6 ka, is in good agreement with the OSL age estimate of 61 ± 2 ka as well as with the U-series result on the calcitic matrix of 82 ± 21 ka. The close agreement of the results suggest that the burial of LM3 took place during the deposition of the upper layers of the Lower Mungo unit, as suggested by Bowler & Thorne (1976).

This dating study demonstrates (1) that it is essential to analyse hominid fossils directly, particularly when their age is beyond the practical limits of radiocarbon dating, and (2) the importance of combining mass spectrometric and gamma spectrometric measurements because only the combination of gamma spectrometric $^{230}\text{Th}/^{238}\text{U}$, $^{226}\text{Ra}/^{230}\text{Th}$ and $^{231}\text{Pa}/^{235}\text{U}$ ratios and mass spectrometric $^{234}\text{U}/^{238}\text{U}$ and $^{230}\text{Th}/^{238}\text{U}$ values allows the recognition of open systems. The best strategy to solve the open system problem for the dating of human remains is the combination of U-series data with ESR analyses of dental material.

We conclude from our dating analyses that the LM3 burial documents the earliest known evidence for physical human presence on the Australian continent.

Implications

Our dating results raise a variety of biological and behavioural issues of regional and wider significance. Lake Mungo is well inland and more than 2700 km from the present northwestern coast of Australia. It is more than 4000 km from the northwestern coast of New Guinea, the northern corner of the Greater Australian continent at that time. That area was nearest the most likely source regions (now Indonesia and the Philippines) for migration to the continent. Therefore, initial colonization may have taken place significantly earlier than an arrival now documented by the LM3 age. Although sea levels in the time range of 60–100 ka were lower than today (by between 20 and 80 m, see Chappell *et al.*, 1996b), it was not a period of major glaciation. Therefore, if the colonization took place after the end of the penultimate glaciation at 130 ka, it suggests that the movement of human groups to Australia had more to do with competent seamanship and appropriate water craft than near-accidental transport across sea gaps (Thorne & Raymond, 1989). In any event, LM3 provides a minimum age for the earliest evidence of human capacity to make significant beyond-the-horizon sea and ocean voyages.

Discussion of the significance of the gracility of the LM3 skeleton depends on a clear definition of its sex. While Bowler & Thorne (1976) initially identified this individual as a male on cranial and postcranial features, Brown (1989, 1994) found its sex *ambiguous* and *problematic*. Apart from the detailed male features identified in Bowler & Thorne (1976), the left femur head has a vertical diameter of 47 mm (it is slightly

eroded and was originally close to 48 mm). Davivongs (1963) found that an Aboriginal femur head diameter of more than 42 mm was male. Further, many Aboriginal people have commented to AT that they have no doubt that LM3 was a burial of a man, given the position of both hand skeletons with their interlocking digits (see Figure 1). Contemporary traditional burial included the positioning of a man's body so that the hands are clasping and protecting the penis, which suggests that such a mortuary practice has a very long prehistory in Australia.

The presence of a modern and gracile morphology at about 60,000 years in Australia, especially given that it predates by some 40,000 years the earliest known of the robust remains from sites such as Kow Swamp, Cohuna, Coobool Creek and the WLH50 individual (Thorne & Wilson, 1977; Thorne, 1980; Brown, 1987, 1989; Simpson & Grün, 1998; Thorne *et al.*, in preparation), is important to the debate over the emergence of modern human variation and the two major explanations for it, the Multiregionalism and recent Out-of-Africa models. Those who see the extremes of Australian Pleistocene skeletal morphology as evidence of the migration of skeletally distinct people from different parts of east and southeast Asia (Thorne & Wolpoff, 1992) will need to explain why gracility appears first in Australia when Indonesia, the nearest source area for migrants, had a long history of robusticity. On the other hand, those who see the LM3 skeletal morphology as indicating the arrival in the western Pacific area of modern human forms, from Africa ultimately (Stringer & McKie, 1996), will need to demonstrate how clear skeletal robusticity developed in Australia over a relatively short period, when gradual gracilization characterizes human evolution over at least the last 200,000 years (e.g., Thorne & Wolpoff, 1992; Stringer & McKie, 1996).

The use of red ochre in the LM3 burial, and a haematite pebble found in the lowermost levels of the Malakunanja II site in Arnhem land at 50–60 ka (Roberts *et al.*, 1990, 1998), indicate that ochre was widely used for artistic and/or philosophical purposes from an early date in Australia.

Acknowledgements

We are particularly grateful to the Aboriginal Community of the Willandra Lakes area for their hospitality, friendship and support of this dating study. We thank the ANU Committee for Major Equipment for their support in establishing the ESR, gamma spectrometric and luminescence dating facilities. J. Monge, University of Philadelphia, provided a doped cast for standard measurements. J. Prescott is thanked for the use of the facilities of the Department of Physics and Mathematical Physics, University of Adelaide, for the measurement of alpha efficiencies, P. Wallbrink and J. Olley, CSIRO, Canberra, for γ -spectrometric analyses and G. Hancock for α -spectrometric analyses. N. Hill, RSES, is thanked for the preparation and measurement of the luminescence samples. We thank J. Olley, Canberra, J. Prescott, University of Adelaide, E. Rhodes, University of London, H. P. Schwarcz, McMaster University, Hamilton, and C. B. Stringer, Natural History Museum, London, for critical comments and Mrs F. M. Grün for corrections. We thank anonymous referees for valuable comments.

References

- Adamiec, G. & Aitken, M. J. (1998). Dose-rate conversion factors: update. *Ancient TL* **16**, 37–50.
- Aitken, M. J. (1994). Optical dating: a non-specialist review. *Quat. Sci. Rev.* **13**, 503–508.
- Aitken, M. J. (1998). *An Introduction to Optical Dating*. Oxford: Oxford University Press.
- Bell, W. T. (1991). Thermoluminescence dates for Lake Mungo fireplaces and the implications for radiocarbon dating. *Archaeometry* **33**, 191–199.

- Bowler, J. M. (1998). Willandra Lakes revisited: environmental framework for human occupation. *Archaeol. Oceania* **33**, 120–155.
- Bowler, J. M. & Price, D. M. (1998). Luminescence dates and stratigraphic analyses at Lake Mungo: review and new perspectives. *Archaeol. Oceania* **33**, 156–168.
- Bowler, J. M. & Thorne, A. G. (1976). Human remains from Lake Mungo: discovery and excavation of Lake Mungo III. In (R. L. Kirk & A. G. Thorne, Eds) *The Origin of the Australians*, pp. 127–138. Canberra: Australian Institute of Aboriginal Studies.
- Bowler, J. M., Thorne, A. G. & Polach, H. A. (1972). Pleistocene man in Australia: age and significance of the Mungo skeleton. *Nature* **240**, 48–50.
- Brennan, B. J., Rink, W. J., McGuirl, E. L., Schwarcz, H. P. & Prestwich, W. V. (1997). Beta doses in tooth enamel by "One Group" theory and the *Rosy* ESR dating software. *Radiation Meas.* **27**, 307–314.
- Brown, P. (1987). Pleistocene homogeneity and Holocene size reduction: the Australian human skeletal evidence. *Archaeol. Oceania* **22**, 47–71.
- Brown, P. (1989). Coobool Creek. *Terra Australis* **13**, 205 p. Canberra: Prehistory ANU.
- Brown, P. (1994). A flawed vision: sex and robusticity on King Island. *Austral. Archaeol.* **38**, 1–7.
- Chappell, J., Head, J. & Magee, J. (1996a). Beyond the radiocarbon limit in Australian archaeology and Quaternary research. *Antiquity* **70**, 543–552.
- Chappell, J., Omura, A., Esat, T., McCulloch, M., Pandolfi, J., Ota, Y. & Pillans, B. (1996b). Reconciliation of late Quaternary sea levels derived from coral terraces at Huon Peninsula with deep sea oxygen isotope records. *Earth Planet. Sci. Lett.* **141**, 227–236.
- Chen, T. M. & Yuan, S. (1988). Uranium-series dating of bones and teeth from Chinese Palaeolithic sites. *Archaeometry* **30**, 59–76.
- Davivongs, V. (1963). The femur of the Australian Aborigine. *Am. J. phys. Anthropol.* **21**, 457–468.
- Gillespie, R. (1997). Burnt and unburnt carbon: dating charcoal and bone from the Willandra Lakes, Australia. *Radiocarbon* **39**, 225–236.
- Grün, R. (1989). Electron spin resonance (ESR) dating. *Quat. Inter.* **1**, 65–109.
- Grün, R. (1995). Semi non-destructive, single aliquot ESR dating. *Ancient TL* **13**, 3–7.
- Grün, R. (1998). Dose determination on fossil tooth enamel using spectrum deconvolution with Gaussian and Lorentzian peak shapes. *Ancient TL* **16**, 51–55.
- Grün, R. & Brumby, S. (1994). The assessment of errors in the past radiation doses extrapolated from ESR/TL dose response data. *Radiation Measurements* **23**, 307–315.
- Grün, R. & Jonas, M. (1996). Plateau tests and spectrum de-convolution for ESR dose determination. *Radiation Measurements* **26**, 621–629.
- Grün, R. & Katzenberger-Apel, O. (1994). An alpha irradiator for ESR dating. *Ancient TL* **12**, 5–38.
- Grün, R. & McDermott, F. (1994). Open system modelling for U-series and ESR dating of teeth. *Quat. Sci. Rev.* **13**, 121–125.
- Grün, R. & Taylor, L. (1996). Uranium and thorium in the constituents of fossil teeth. *Ancient TL* **14**, 21–25.
- Grün, R., Schwarcz, H. P. & Chadam, J. M. (1988). ESR dating of tooth enamel: coupled correction for U-uptake and U-series disequilibrium. *Nucl. Tracks Radiation Meas.* **14**, 237–241.
- Grün, R., Yan, G., McCulloch, M. & Mortimer, G. (1999). Detailed U-series analyses of teeth, implications for uranium migration and dating. *J. Archaeol. Sci.*, in press.
- Huntley, D. J., Godfrey-Smith, D. I. & Thewalt, M. L. W. (1985). Optical dating of sediments. *Nature* **313**, 105–107.
- Huxtable, J. & Aitken, M. J. (1977). Thermoluminescence dating of Lake Mungo geomagnetic polarity excursion. *Nature* **265**, 40–41.
- Longtin, J. P. (1988). Occurrence of radon, radium, and uranium in groundwater. *J. Am. Water Works Assoc.* **80**, 84–93.
- Ludwig, K. R. & Titterton, D. M. (1994). Calculation of $^{230}\text{Th}/\text{U}$ isochrons, ages, and errors. *Geochim. Cosmochim. Acta* **58**, 555–564.
- McDermott, F., Stringer, C., Grün, R., Williams, C. T., Din, V. K. & Hawkesworth, C. J. (1996). New Late-Pleistocene uranium-thorium and ESR dates for the Singa hominid (Sudan). *J. hum. Evol.* **31**, 507–516.
- Osmond, J. K. & Ivanovich, M. (1992). Uranium series mobilization and surface hydrology. In (M. Ivanovich & R. S. Harmon, Eds) *Uranium Series Disequilibrium, Applications to Earth, Marine, and Environmental Sciences*, pp. 259–289. Oxford: Clarendon Press.
- Oyston, B. (1996). Thermoluminescence age determinations for the Mungo III human burial, Lake Mungo, southeastern Australia. *Quat. Sci. Rev.* **15**, 739–749.
- Prescott, J. R. & Hutton, J. T. (1994). Cosmic ray contributions to dose rates for luminescence and ESR dating: large depths and long-term time variations. *Radiation Meas.* **23**, 497–500.
- Prescott, J. R., Huntley, D. J. & Hutton, J. T. (1993). Estimation of equivalent dose in thermoluminescence dating—the Australian slide method. *Ancient TL* **11**, 1–5.
- Questiaux, D. G. (1990). Optical dating of loess: comparisons between different grain size fractions for infrared and green excitation wavelengths. *Nucl. Tracks Radiation Meas.* **18**, 133–139.
- Readhead, M. L. (1984). Thermoluminescence dating of some Australian sedimentary deposits. Unpublished Ph.D. Dissertation, Australian National University.
- Readhead, M. L. (1988). Thermoluminescence dating study of quartz of aeolian sediments from southeastern Australia. *Quat. Sci. Rev.* **7**, 325–329.
- Rees-Jones, J. & Tite, M. S. (1997). Optical dating results for British archaeological sediments. *Archaeometry* **39**, 177–187.
- Roberts, R. G., Jones, R. & Smith, M. A. (1990). Thermoluminescence dating of a 50,000 year old human occupation site in northern Australia. *Nature* **345**, 153–156.

- Roberts, R., Yoshida, H., Galbraith, R., Lastett, G., Jones, R. & Smith, M. (1998). Single-aliquot and single grain optical dating confirm thermoluminescence age estimates at Malkunanja II rock shelter in northern Australia. *Ancient TL* **16**, 19–24.
- Schwarcz, H. P. (1980). Absolute age determination of archaeological sites by uranium-series dating of travertine. *Archaeometry* **22**, 3–25.
- Schwarcz, H. P. (1997). Uranium series dating. In (R. E. Taylor & M. J. Aitken, Eds) *Chronometric and Allied Dating in Archaeology*, pp. 159–182. New York: Plenum.
- Simpson, J. J. & Grün, R. (1998). Non-destructive gamma spectrometric U-series dating. *Quat. Sci. Rev.* **17**, 1009–1022.
- Spooner, N. A., McBryde, I., Magee, J. W., Lawson, G., Williams, L., Johnston, H., Clark, P., Questiaux, D. G., Olley, J. M. & Hill, N. (in preparation). Optical dating at Lake Mungo: evidence for early human occupation.
- Stirling, C. H., Esat, T. M., McCulloch, M. T. & Lambeck, K. (1995). High precision U-series dating of corals from western Australia and implications for the timing and duration of the Last Interglacial. *Earth and Planetary Science Letters* **135**, 115–130.
- Stringer, C. & McKie, R. (1996). *African Exodus*. London: Jonathan Cape.
- Thorne, A. G. (1980). The longest link: human evolution in Southeast Asia and the settlement of Australia. In (J. J. Fox, A. G. Garnaut, P. T. McCawley & J. A. C. Maukie, Eds) *Indonesia: Australian Perspectives*, pp. 35–43. Canberra: Australian National University.
- Thorne, A. G., Grün, R., Spooner, N., Simpson, J. J. & McCulloch, M. (in preparation). The age of WLH 50.
- Thorne, A. & Raymond, R. (1989). *Man on the Rim*. Sydney: Angus and Robertson.
- Thorne, A. & Wilson, S. (1977). Pleistocene and recent Australians: a multivariate comparison. *J. hum. Evol.* **6**, 393–402.
- Thorne, A. G. & Wolpoff, M. H. (1992). The multi-regional evolution of humans. *Sci. Am.* **266**, 76–83.
- Yang, Q. (1997). Experimental determination of beta attenuation in tooth enamel layers and its implication in ESR dating. Unpublished M.Sc. Thesis, McMaster University.